13th World Conference on Earthquake Engineering
Vancouver, B.C., Canada
August 1-6, 2004
Paper No. 91

EXPERIMENTAL AND ANALYTICAL INVESTIGATION OF REPAIRED AND STRENGTHENED REINFORCED CONCRETE STRUCTURAL ELEMENTS UTILIZING CFRP

G.C. MANOS [1], D.S. STAVROY[2], M. A. DIMOSTHENOUS[3], B. KOURTIDES[4]

SUMMARY

This research aimed to investigate the ultimate behaviour of Reinforced Concrete structural elements such as columns and beams repaired with Carbon Fiber Reinforced Plastic (CFRP) sheets. The whole investigation was conducted utilizing simple loading arrangements on concrete cylinders as well as on Reinforced Concrete beams and columns. The experimental investigation was carried out at the Laboratory of Strength of Materials at the University of Thessaloniki. The number of specimens was limited but sufficient to allow the study of the applicability of FRP sheets and the examination of the specimens' behaviour up to failure. The observed measurements were compared with predictions obtained from analytical relations suggested from other researchers, which are broadly used. The Reinforced Concrete column specimens were tested under axial compression up to failure, where destruction of the central core of concrete, buckling of the longitudinal reinforcement and local fracture of transverse reinforcement occurred. These specimens were repaired using CFRP sheets and the same loading procedure was repeated. The Reinforced Concrete beams were subjected to three points flexure up to failure of the specimen. After failure, the beam specimens were also repaired by CFRP and the same loading procedure repeated. The repaired column specimens showed: a) restored or even increased load-carrying capacity, b) reasonably good post elastic behaviour c) agreement between measured and predicted values. The repaired beam specimens demonstrated that a) proper application of FRP sheets with the guidance of analytical predictions of shear and bending moment capacities can ensure that desired mode of failure does develop whereas the undesirable modes of failure, which we aim to suppress, can be prohibited b) depending on the M / (V d) ratio value, the shear capacity prediction seems to be the one with the largest degree of uncertainty.

1. INTRODUCTION

The use of fiber reinforced plastics (FRP's) in the repair and strengthening of reinforced concrete (R.C.) structures damaged by earthquakes is being widely promoted. As main advantages of such a repair

[1] Professor, Laboratory of Strength of Materials, Department of Civil Engineering, Thessaloniki 54006, tel.: 2310995657, fax: 2310995769, email: gcmanos@civil.auth.gr
[2] Researcher, Civil Engineer, Department of Civil Engineering.
[3] Researcher, I.T.S.A.K., Dr Civil Engineer.
[4] Civil Engineer

technique one can note that its application is relatively easy; moreover, an upgraded strength can be achieved in certain cases for R.C structural members repaired by FRP's. Thus, for repairing damaged structural members the application of FRP's can be a competitive proposition when compared to other traditional repair and strengthening techniques (e.g. concrete or steel jacketing). Despite this, it must be mentioned that the repair by FRP's is a relatively new technique and it must be used with caution regarding its durability; moreover, the sensitivity of its performance to earthquake loading must be substantiated by more experimental data on actual repaired structural members subjected to combined gravity and earthquake loads. This work is based on an experimental investigation that examines the behavior of reinforced concrete (R.C.) column or beam specimens under simple static loading conditions. The columns are subjected to axial compression whereas the beams are subjected to flexure and shear. A number of column and beam specimens are tested first in their initial virgin condition up to limit levels where a certain mode of damage is well developed. Then, these damaged specimens are repaired in certain ways, which also include the use of Carbon FRP sheets, and are tested again as will be described below. The main objectives are:

- For the columns with square cross-section: to study the degree of confinement that is provided by the CFRP to the repaired specimens and to compare the compressive bearing capacity of the repaired specimen with that of the virgin column specimen.
- For the beams: to investigate whether the repair technique using CFRP can influence the type of failure mode of the repaired specimen; in addition, to compare the shear or the bending strength of the repaired specimen with the corresponding strengths of the virgin beam specimen.
- For both the column and beam specimens (virgin and repaired by CFRP): to compare the observed bearing capacities with predictions made through analytical approaches proposed by other researchers, thus validating the applicability of such approaches.

2 EXPERIMENTAL INVESTIGATION.

2.1. Simple Tests.

Initially, a series of tensile tests of the employed CFRP sheets were conducted that resulted in ultimate strength $\boldsymbol{\sigma_u}$ **= 2013.9 Mpa** for a strain equal to ε_u=1%, Young's modulus $\mathbf{E_f}$ **= 223.2 GPa** and observed elastic behavior almost all the way to failure. It must be noted that the used CFRP sheets had fibers oriented in one axis, which corresponds to the tensile properties given above. Next, two groups of three cylindrical concrete specimens each were utilized. These cylindrical specimens had 150mm diameter and 300mm height, and each group was cast on the same day. The first specimen of the first and second groups resulted in an unconfined compressive strength of 26.1 Mpa and 29.7 Mpa, respectively, tested 28 days after their casting date. The second and third specimens of each group were tested immediately afterwards, having one and two layers of CFRP respectively. Apart from the axial compressive load, the axial and transverse deformation was monitored for these specimens as can be seen in figures 1 and 2. This was done for the first group specimens by monitoring the change of the diameter of the cylinder in two horizontal orthogonal directions; this was also repeated for the specimens of the second group whereby the transverse strain was also monitored by strain gauges. Summary results are also presented in Tables 1,2 together with predicted values from applying empirical formulae 1, 2, 3.
For the specimens of the first group, apart from the considerable increase in the strength provided by the CFRP confinement, the two layer CFRP cover resulted in considerable axial strain levels (6%). This was also observed for the second group specimens; however, this time the axial strain level increase was modest (2.5% for the two layer case). The one layer confinement is less effective as the scenario of slip may also occur if the overlap of the edges of the CFRP is not sufficiently long. The increase in the measured strength provided by the CFRP confinement is quite noticeable from the observed strengths for the specimens of both groups. The one or the two-CFRP layers results in a confined strength almost twice or three times the unconfined strength value, respectively. The measured maximum transverse strains (1-

1.5%) for the specimens of both groups are of the same level as the one measured during the uni-axial tensile tests of the CFRP sheet specimens.
The expression proposed by Pauley and Priestley (1992) for cylindrical specimens confined by spiral steel reinforcement was modified and assumed to be applicable to the confinement provided by the CFRP, as is explained below.

$$\mathbf{f_{cc}=\left[-1{,}254+2{,}254\sqrt{1+7{,}94\frac{f_l}{f_c}}-2\frac{f_l}{f_c}\right]f_c} \qquad \textbf{(1)}$$

$$\mathbf{\varepsilon_{cr}=0.002\left[1+5\left(\frac{f_{cc}}{f_c}-1\right)\right]} \qquad \textbf{(2)}$$

f_{cc} : the strength of the confined concrete
f_c : the strength of the unconfined concrete
ε_{cr} : the axial strain at ultimate compressive stress (f_{cc}).
f_l : the confinement stress given as $f_l = k * \rho * f_y$
k Coefficient of uniformity taken as k=1 for the confinement provided by the CFRP.
f_y Initially the yield stress for confinement provided by steel stirrups. The ultimate strength (f_{ufrp}) of CFRP as it remains elastic even for strains equal to 1%. An alternative definition can be based on a strain limitation.

$\rho=\dfrac{n * Aw}{dx * Sw}$, The transverse reinforcement ratio
dx the length of the confined area
Sw the distance between consecutive stirrups
n * Asw The total area of a number (n) of stirrups active in one direction.

According to the above the confinement stress provided by the layers of CFRP is equal to:

$$\mathbf{f_l=\frac{2 * f_{ufrp}}{D * S}Asw}\ ,$$

D : the diameter of the cylindrical specimen
Asw : the area of the CFRP sheet equal to **t * S**
t : the thickness of the CFRP sheet. In cases when the confinement is provided by a multilayer CFRP cover, the thickness of one layer is multiplied by the number of layers.
S: The length of the CFRP sheet (in the case of the cylindrical specimen the height of the cylinder)

An alternative expression (equation 3) of the FRP confined ultimate compressive stress confinement is proposed by Pantazopoulou (2000). The symbols f_{cc} , f_c , **D, t,** n have the same definition given for equations 1 and 2 above.

$$\mathbf{f_{cc}=f_c+3\left(2t\,E_{frp}\,\varepsilon_{axial}\frac{n}{D}\right),\ \ \sigma_{FRP}=E_{FRP}\cdot\varepsilon \Rightarrow\ f_{cc}=f_c+3\left(2\sigma_{frp}\,t\frac{n}{D}\right)} \qquad \textbf{(3)}$$

E_{frp} : the Young's modulus for FRP.
σ_{FRP} : the direct tensile strength of a FRP specimen. .
n : the number of FRP layers.

Based on the above expressions and on the values of the various parameters corresponding to the two groups of cylindrical specimens confined by CFRP described above, predictions of ultimate compressive strength and corresponding strains values were derived; these are listed in tables 1 and 2 and plotted in figures 1 and 2.
The following summarize the most important observations derived from the measured and predicted values of these simple compression tests:

- For the specimens of the first group, the predictions of the confined strength underestimate the observed values. This is quite noticeable for the specimens with two layers of CFRP and for the predicted values employing expression 3, which in this way results in conservative predictions.
- At ultimate compressive stress, the predicted axial strain value is underestimated for both CFRP specimens of group 2 (figure 2) and overestimated for both CFRP specimens of group 1 (figure 1).

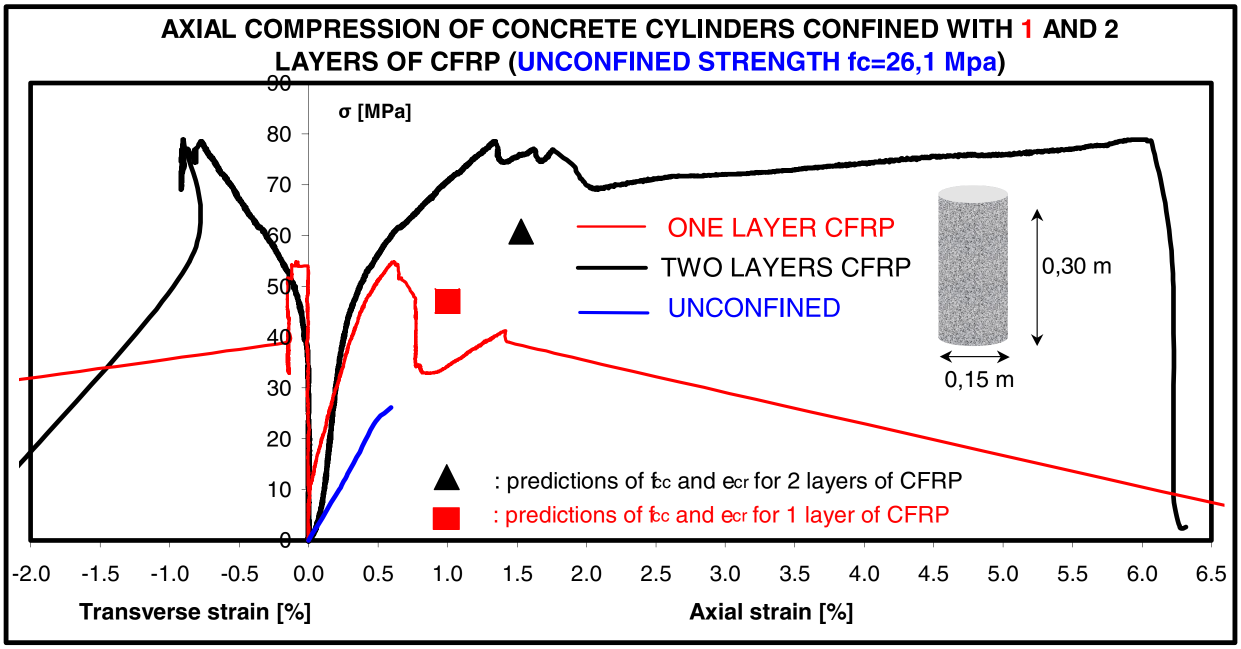

Figure 1. Axial compression tests of cylindrical specimens with or without CFRP confinement

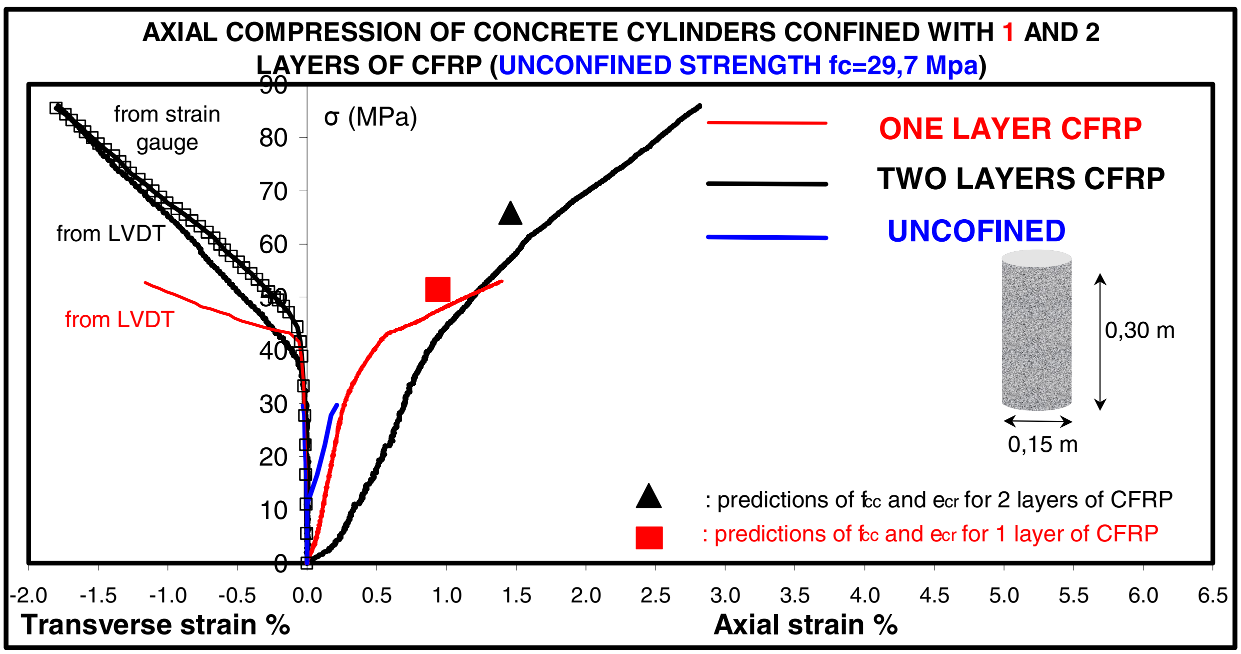

Figure 2. Axial compression tests of cylindrical specimens with or without CFRP confinement

Table: 1. Compressive strength of concrete cylinder specimens confined with CFRP

COMPRESSIVE STRENGTH OF UNCONFINED CONCRETE f_c (MPa)	LAYERS OF CFRP	**COMPRESSIVE STRENGTH OF SPECIMENS CONFINED WITH CFRP** f_{cc} (MPa)				
		Experimental measurements	Equation 1	**Ratio: Exp/Eq. 1**	Equation 3	**Ratio: Exp/Eq. 3**
26.1	1	**54.85**	47.18	**1.25**	38.99	**1.41**
26.1	2	**78.83**	60.79	**1.30**	51.87	**1.52**
29.7	1	**53.02***	51.42	**1.03**	42.62	**1.24**
29.7	2	**86.05**	65.89	**1.31**	55.50	**1.55**

* Slip failure of the CFR layer was observed.

Table: 2. Axial strain of concrete cylinder specimens at the maximum compressive strength level.

COMPRESSIVE STRENGTH OF UNCONFINED CONCRETE f_c (MPa)	LAYERS OF CFRP	AXIAL STRAIN AT MAXIMUM COMRESSIVE STRENGTH FOR SPECIMENS CONFINED WITH CFRP ε_{cr} (‰)		
		Experimental measurements	Equation 2	**Ratio: Exp/Eq 2**
26.1	1	**6.25**	10.4	**0.60**
26.1	2	**13.5**	15.7	**0.86**
29.7	1	**14.0**	9.4	**1.50**
29.7	2	**27.5**	14.6	**1.88**

2.2. Column specimens subjected to axial compression.

2.2.1. Initial Virgin specimens.

These specimens had a square cross-section 200mm x 200mm with 4 corner longitudinal reinforcing bars of 20mm diameter (total area As=12,57cm^2) and 8mm diameter stirrups spaced every 100mm along the height of the column, equal to 1360mm. These specimens were subjected to axial compression up to failure. Certain measures were taken so that the compressive failure developed at the middle 1/3 of the height of the specimen and was accompanied by the buckling of the longitudinal reinforcement, the opening or fracture of the stirrups and the crushing of the largest part of the concrete core. Results from two specimens are presented here. The code name of these virgin specimens is CAJ3 and CAC2.

2.2.2. Columns repaired by high strength concrete.

As a first step towards the repair of these damaged columns, the buckled longitudinal reinforcement was cut so that it became totally ineffective and the same was done for the damaged stirrups. No attempt was made at this stage to repair the damaged reinforcement; this will be investigated in a future experimental sequence. Next, the initial geometry of the specimen was secured and all the damaged concrete part was removed. Finally, high strength and low shrinkage concrete (EMACO) was cast at the damaged central 1/3 part of the column and was cured for 20 days. These repaired specimens were tested again to axial compression up to failure. At the time of the compressive tests with these repaired columns, tests were also conducted on cylindrical specimens taken from the high strength concrete used in the repair during casting. The corresponding unconfined compressive strength of these high strength concrete specimens was 41.6 MPa and 50.0 MPa, for the mixture used in the repair of CAJ3 and CAC2, respectively.

2.2.3. Columns repaired by high strength concrete and CFRP.

The failed specimens, described in 2.2.2., were repaired again by removing all the crushed high strength concrete central 1/3 portion. Next, high strength concrete was again cast in this portion. Moreover, after rounding the corners of this central portion (rounding radius r=30mm), a number of layers of CFRP were applied. In one case 1 layer of CFRP was employed whereas in the second case 2 layers of CFRP were used, thus corresponding to the number of layers utilized in the simple test sequence described in 2.1. The code name of these specimens repaired by CFRP, corresponding to the virgin column specimens CAJ3 and CAC2, is CAJR3 and CACR2, respectively.

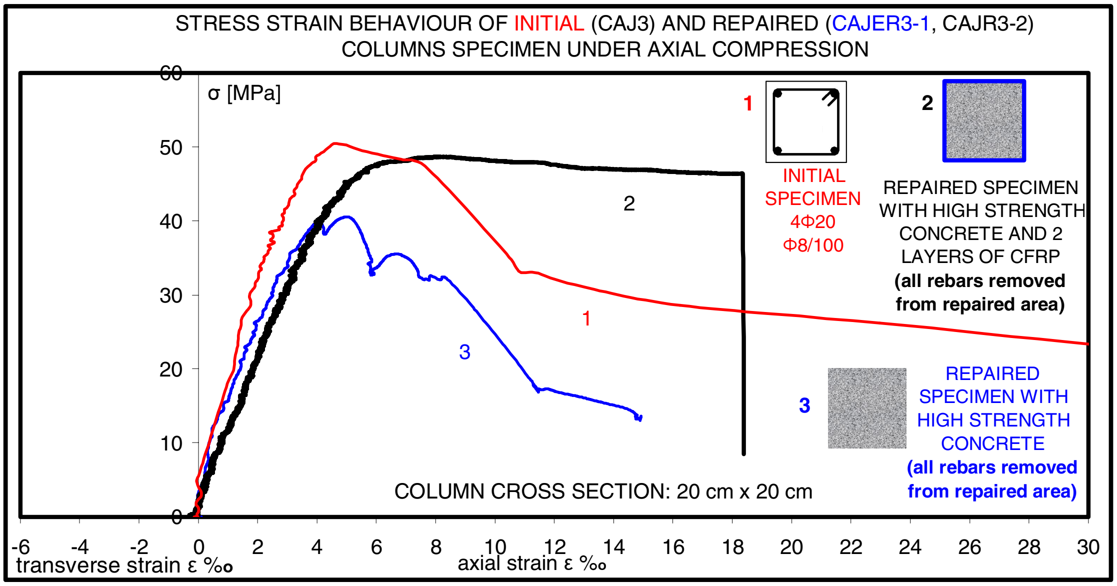

Figure: 3. Repaired column CAJR3 (unconfined strength of high strength concrete: f_c=41.6 MPa).

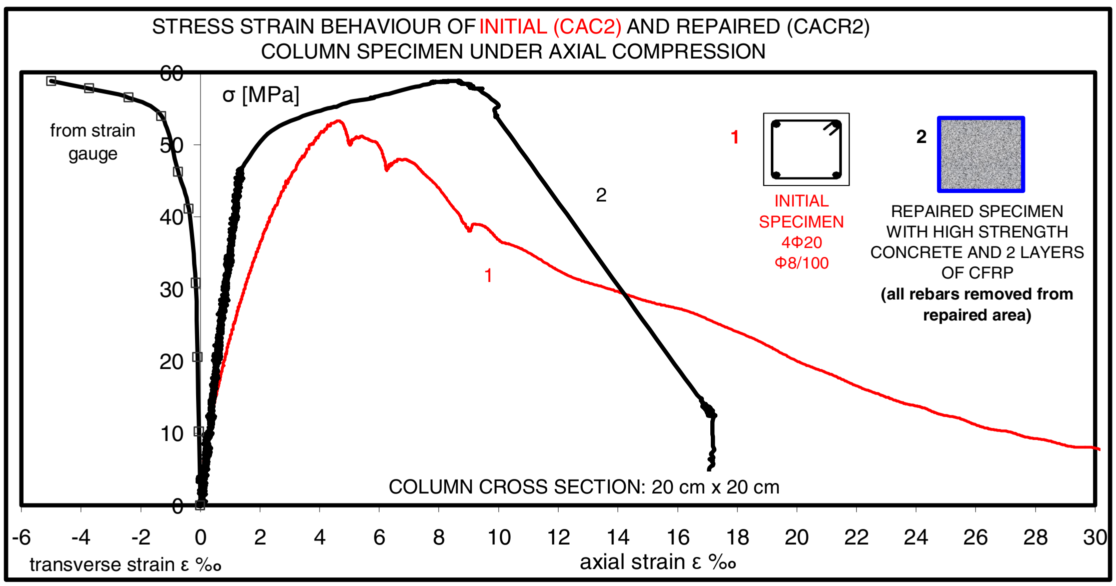

Figure: 4. Repaired column CACR2 (unconfined strength of high strength concrete: f_c=50.0 MPa)

2.2.4. Obtained results.

The obtained results are depicted in figures3 and 4 in terms of axial stress and axial and transverse strain diagrams. The axial stress resulted from the measured axial load, assuming uniform distribution on the total cross-section. The axial strain was derived from monitoring the axial deformation of the central 1/3 portion of the specimen with displacement transducers, which were placed along each one of the four sides of the tested column. The plotted value is the average of all four recorded axial deformations. The transverse strain was measured for the specimens with the CFRP using strain gauges. The measured results are plotted in figures 3 and 4 and listed in tables 3 and 4 together with predictions based on equations 1, 2, 3 as was done in section 2.1. In this case, applying equation 1, the coefficient of uniformity was assumed to have the value k=0.75.

The following are the main observations that were derived from the performed tests:

- As was expected, the CFRP confinement resulted in larger compressive strength values than the corresponding values of the column specimens repaired by high strength concrete without CFRP confinement.
- The repaired CAJR3 performance, even without longitudinal reinforcement, had almost the same strength as the original virgin specimen and retained the bearing capacity for larger levels of axial strain than the virgin specimen.
- The repaired CACR2 performance, even without longitudinal reinforcement, exhibited higher strength levels than the original virgin specimen and retained the bearing capacity for almost the same levels of axial strain as the virgin specimen.
- The maximum transverse strain measured at the outside surface of the CFRP layer at the middle of one side of the CACR2 specimen was at the level of 0.5% (half the maximum axial strain value measured for the same type of CFRP during the initial uni-axial tension experiments). However, it must be noted here that the failure of the CFRP confinement for the CACR2 specimen developed at the corners and was not due to direct tension. This indicates that the shaping of the corner for the repaired specimen prior to the application of the CFRP sheets is very important. The use in this case of a rounding radius at the corners equal to r=30mm was not sufficient.
- For both column specimens, the CFRP confined compressive strength is underestimated by the predicted values utilizing both expressions 1 and 3.
- The axial strain value at ultimate compressive stress is successfully predicted for both specimens (equation 2).

Table 3. Compression strength of column specimens confined with CFRP.

SPECIMEN WITH TWO LAYERS CFRP	COMPRESSIVE STRENGTH OF EMACO f_c (MPa)	COMPRESSIVE STRENGTH OF SPECIMENS CONFINED WITH CFRP f_{cc} (MPa)				
		Experimental measurements	Equation 1	**Ratio: Exp./Eq. 1**	Equation 3	**Ratio: Exp./Eq. 3**
CAJR3	41.6	**49.95**	68.18	**0.73**	60.93	**0.82**
CACR2	50.0	**58.94**	77.50	**0.76**	69.33	**0.85**
CACR2*	50.0	**58.94**	65.00	**0.91**	59.67	**0.99**

* The assumption for this set of values is that the confined stress is based on the strain value measured by the strain gauge attached on the CFRP surface. This is $\varepsilon_{\alpha v} = 0{,}55\ \% < \varepsilon_u = 1\ \%$ (figure 4).

Table 4. Axial strain at ultimate compression strength of column specimens confined with CFRP.

SPECIMEN WITH TWO LAYERS CFRP	COMPRESSION STRENGTH OF EMACO f_c (MPa)	AXIAL STRAIN AT MAXIMUM COMRESSION STRENGTH OF SPECIMENS CONFINED WITH CFRP ε_{cr} (‰)		
		Experimental measurements	Equation 2	Ratio: Exp/Eq 2
CAJR3	41.6	8.35	8.39	1.00
CACR2	50.0	8.02	7.50	1.07

2.3. Beam specimens subjected to flexure and shear.

All the tested beam specimens were subjected to three point flexure either in their initial virgin condition or after repair, as is explained below. The span as well as the distance from the nearest support of the point where the concentrated load was applied were variables; this was done in order to selectively vary the amplitude of the shear and bending moment demands from specimen to specimen as well as the M / (V d) ratio (see figures 5, 6, 8, 9, 11, 13). For all tests, apart from monitoring the variation of the applied load, the deformations of each specimen were also recorded by measuring the deflections at mid-span and under the points of application of the concentrated loads. From the applied load, the shear (Q) and bending moment (M) demands could be derived.

2.3.1. Initial Virgin specimens.

These specimens had a rectangular cross-section 200mm width and 300mm height and a total length of 3100mm. They were reinforced with 4 corner longitudinal reinforcing bars of 20mm diameter (total area

$As=12,57cm^2$). Thus, during the loading of the beam specimens in flexure and shear, two of the rebars were located in the tensile area whereas the other two in the compression area. Rectangular stirrups of 8mm diameter were spaced every 100mm along the total length of these beam specimens. The code name of these virgin specimens is BAJ1, BAJ2, BAC2 and BAC3. Two of these specimens were loaded in their initial virgin condition up to failure (BAJ1 and BAC2). The mode of failure that developed in these specimens is mainly flexural and limited shear for BAC2 whereas for BAJ1 the shear failure was more predominant. The repair of these specimens involved the replacement of all the damaged concrete areas by low-shrinkage high strength concrete as well as the application of CFRP sheets, as will be explained in schemes 1 and 2 below. The code name of these beam specimens repaired by CFRP, corresponding to the virgin beam specimens BAJ1 and BAC2, is BAJR1 (repaired by CFRP in shear) and BACR2 (repaired both in shear and in flexure).

The beam specimens BAJ2 and BAC3 were tested in their virgin state but with CFRP sheets applied on them from the beginning, as will be explained below.

2.3.2. Beams repaired by high strength concrete and CFRP.

The damaged beam specimens, described in 2.3.1., were repaired again by removing all the damaged concrete regions in shear. The cracked concrete in the parts of the beam deformed by flexure were left untouched. Permanent flexural deformations were removed by reverse loading. The longitudinal reinforcement was left untouched, even the rebars that may have yielded. There was no fracture of any longitudinal reinforcement. Deformed transverse reinforcement was repositioned without replacement. Next, high strength concrete (EMACO) was cast in all the portions of the beam specimens where the damaged concrete was removed. The application of CFRP layers was done in three distinct ways.

- <u>Scheme 1.</u> In order to upgrade the shear capacity of the parts of the beams that sustained shear damage, the CFRP layers were applied with the axis of the fibers perpendicular to the axis of the beam. The CFRP sheets in this case covered the beam from all sides without interruption and with an overlap equal to the beam's height (300mm). The length of these sheets extended towards the mid-span beyond the point of the application of the concentrated loads, as depicted in figures 6, 9, 11. This scheme was used for repaired specimens BAJR1 (figures 6, 7) and BACR2 (figures 9,10) and for virgin specimens BAC3-1 and BAC3-2 (figures 11,12). In all the cases where the CFRP sheets were applied surrounding the beam sections in this way (schemes 1 and 3), a rounding of the corners (with rounding radius r=30mm) of the corresponding beam portion was done prior to the application of the CFRP sheets.
- <u>Scheme 2.</u> In order to repair and strengthen the beam specimens damaged in flexure, layers of CFRP were attached at the bottom side of these specimens with the axis of the fibers parallel to the longitudinal axis of the beam. These CFRP layers had a width equal to the width of the beam (200mm) and a length that extended from mid-span symmetrically towards the supports as indicated in the corresponding figures 9,11. This scheme was utilized for repaired specimen BACR2 (together with scheme 1), as can be seen in figures 9,10. It was also applied in virgin specimen BAC3-1 and BAC3-2 together with scheme 1 (fig.11,12). For specimen BAC3-1 this bottom side CFRP sheet extended 220mm beyond the point of application of the concentrated load towards the support of the beam (very short anchorage); this flexural CFRP sheet was attached first and then the shear CFRP attachment (scheme 1) was done. For this specimen the flexural failure was accompanied with the slip of the CFRP bottom side sheet from the bottom side concrete surface. This specimen was repaired again by removing the slipped CFRP sheet, by rotating the specimen upside down and by attaching a new flexural CFRP sheet at the bottom side (specimen BAC3-2, figure 11); this time, the bottom side CFRP sheet extended from mid-span all the way to the supports (660mm beyond the point of applying the concentrated load towards the support). Moreover, this time the flexural CFRP bottom side sheet was attached on top of the already existing shear type CFRP attachment (Scheme 1).
- <u>Scheme 3.</u> In one case (virgin specimen BAJ2) a shear type CFRP attachment was applied at the central portion of the beam prior to any loading, similar to the one described in scheme 1 (e.g. with the axis of the fibers perpendicular to the axis of the beam). However, this time the aim was to increase the confinement of the concrete at the compressive zone (figures 13,14) and thus to avoid the type of flexural mode of failure which is accompanied with the crushing of the concrete in the upper compressive zone of the beam.

2.3.3. Predictions of shear and flexural capacity based on expression proposed by other researchers.

a) The shear capacity of the beam was derived based on approaches proposed by Kani 1966, Zsutty 1968, Pauley and Priestley 1992, Zararis 2002, and the Greek Code for R.C. Structures (without safety factor, ΕΚΩΣ-2000). In all these approaches, it is assumed that shear cracks have developed. The contribution of the attached CFRP was incorporated in a simple way assuming full compatibility of the CFRP sheet with the R.C. section and utilizing the measured mechanical characteristics for the CFRP. The total shear capacity of the beam section (**V_R**) is the sum of contributions from the compressive zone concrete and the dowel action of the longitudinal reinforcement (**Vc**), the contribution of the stirrups (**Vw**) and the contribution of the CFRP (**V_{frp}**). Only Vc can be derived by either the Kani or Zsutty approach. In this case, in order to reach a value of the total shear capacity, the values for Vw, predicted by Priestley and Pauley, are also adopted here. The comparison of the predicted and observed values is listed in Tables 5 (for BAJR1), 6 (for BACR2) and 7 (BAC3-1, BAC3-2). A comparison of the variation of the observed shear demand during the loading sequence with the predicted shear capacity by the various approaches is done in figure 5 (BAJ1), in figure 6 (BAJR1), in figure 8 (BAC2), in figure 9 (BACR2), in figure 11 (BAC3-1, BAC3-2) and in figure 13 (BAJ2).
b) Two levels of bending moment capacity were derived; the first corresponds to the yield moment (**My**) and is based on a measured yield stress for the longitudinal reinforcement **fy**=545Mpa whereas the second is the bending strength (**Mu**) and is based on the measured ultimate tensile strength of the longitudinal reinforcement equal to **fu**=660Mpa. A comparison of the variation of the observed bending moment demand during the loading sequence with the predicted bending moment capacity is done; figure 7 (BAJ1, BAJR1), figure 10 (BAC2, BACR2), figure 12 (BAC3-1, BAC3-2) and figure 14 (BAJ2).

2.4. Discussion of the observed and predicted behavior
All the following plots depict the variation of a measured demand quantity (shear force Q or bending moment M) against the corresponding measured mid-span deflection (δ). Within the same plots, the predicted shear force or bending moment demand levels are also depicted with constant lines.
2.4.1 Virgin specimen failed in shear (BAJ1) and repaired specimen (BAJR1) to avoid shear failure.

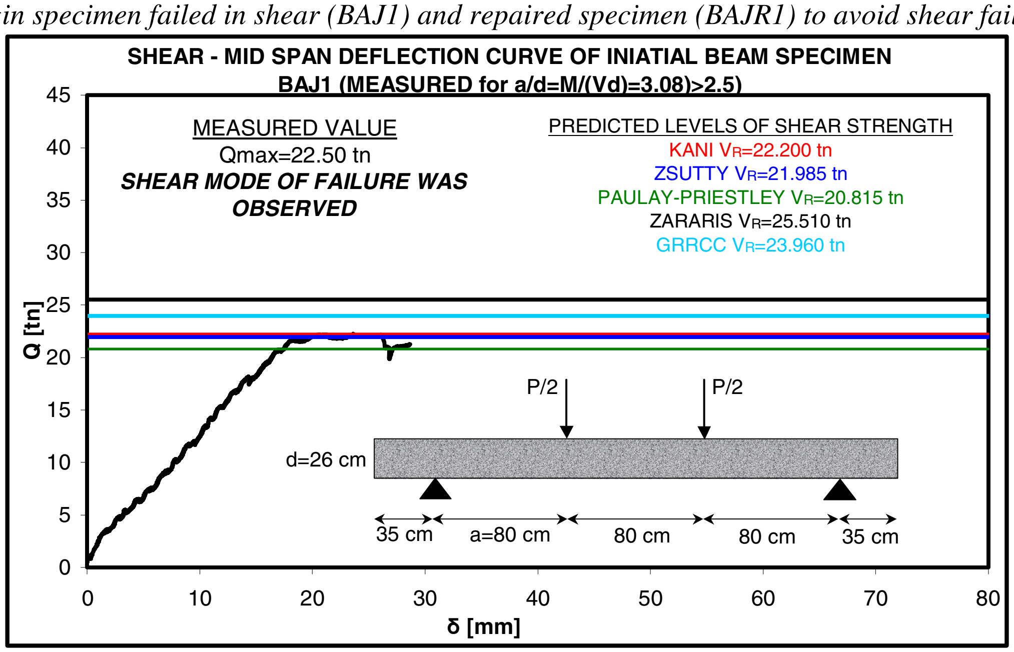

Figure 5. Comparison between observed shear demand and predicted shear capacity (BAJ1)
The initial specimen BAJ1 failed mainly in shear mode. This is predicted by Kani, Zsutty and Paulay and Priestley in figure 5. The Greek code and Zararis predictions overestimate the shear capacity. Moreover, the applied repair by the CFRP (scheme 1) was successful in prohibiting the shear mode of failure, as can be seen in figure 6. This is again predicted by all the approaches including the contribution of the CFRP,

also depicted in figure 6. It can also be observed that the virgin specimen BAJ1 failed prematurely below its bending moment strength (having exceeded the yield moment) whereas the repaired against shear specimen BAJR1, although developing approximately the same shear demand as before, failed in flexure in a ductile manner having reached the ultimate bending strength prediction (figure 7).

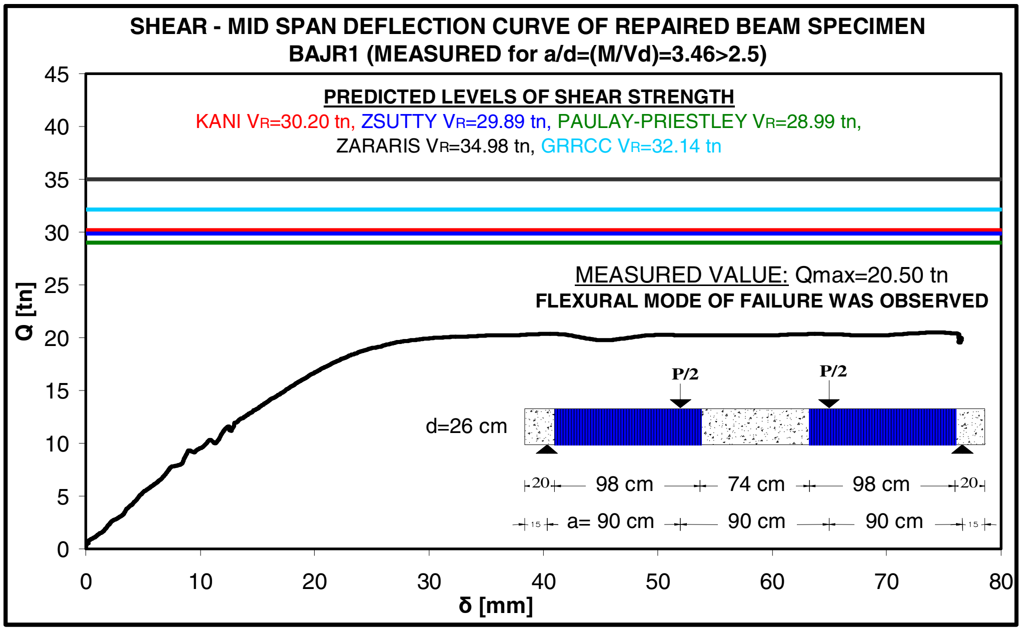

Figure : 6. Comparison between observed shear demand and predicted shear capacity (BAJR1)

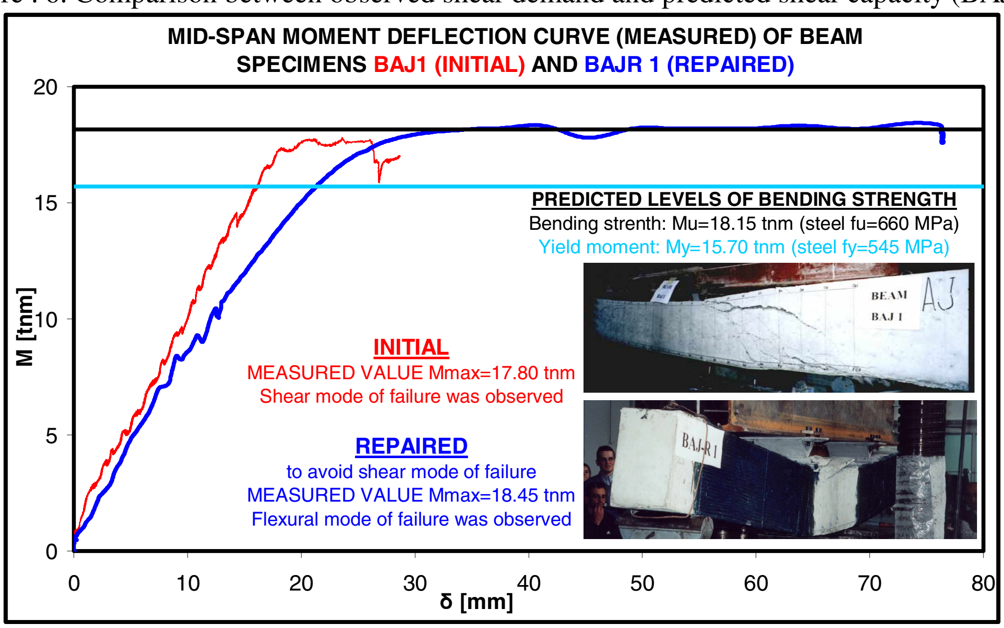

Figure 7. Comparison between observed flexural demand and predicted flexural capacity (BAJ1-BAJR1)

2.4.2. Virgin specimen BAC2 (failed mainly in flexure and shear) and repaired specimen BACR2

The observed, mainly flexural, failure of the virgin specimen BAC2 is reasonably well predicted (the demand exceeded the yield moment, figure 10). The secondary shear failure was not predicted by all approaches (figure 8). The repaired specimen, utilizing a combination of repair schemes 1 and 2 with CFRP, was aimed at enforcing shear failure on the CFRP repaired region (Scheme 1). This was successful as the repaired specimen was observed to fail in shear at the region repaired by CFRP. This is reasonably well predicted by all approaches, except by the one proposed by Kani. The predictions by Zararis or by Paulay and Priestley seem to be more successful this time. It must be pointed out that the M/Vd ratio for BAC2R is equal to 1.73 (M/Vd <2.5) whereas for specimens BAJ1 and BAJR1 this ratio is equal to 3.08 and 3.46 (M/Vd >2.5), respectively.

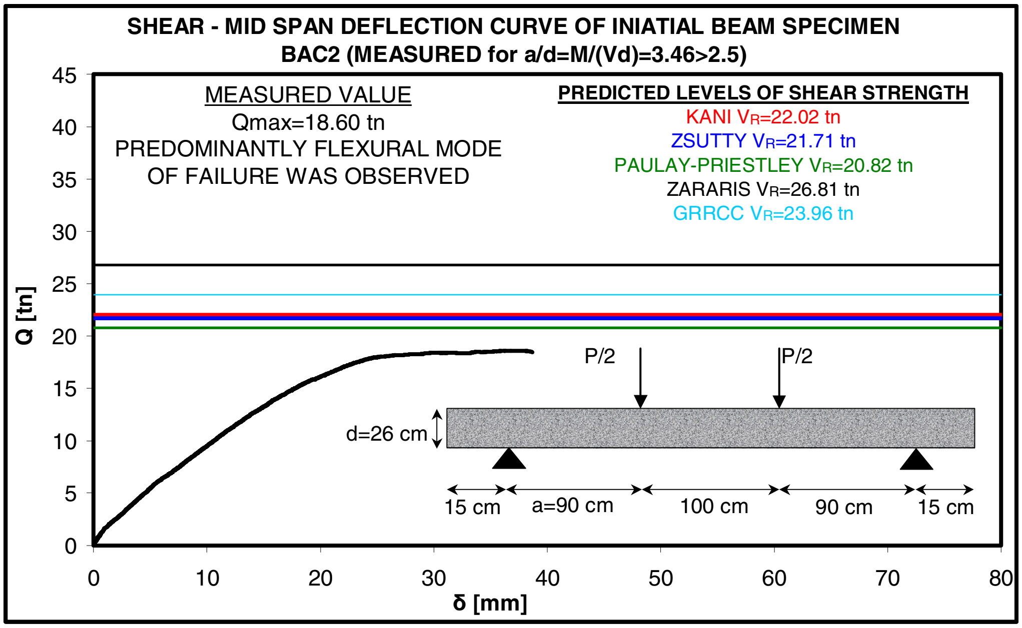

Figure : 8. Comparison between observed shear demand and predicted shear capacity (BAC2)

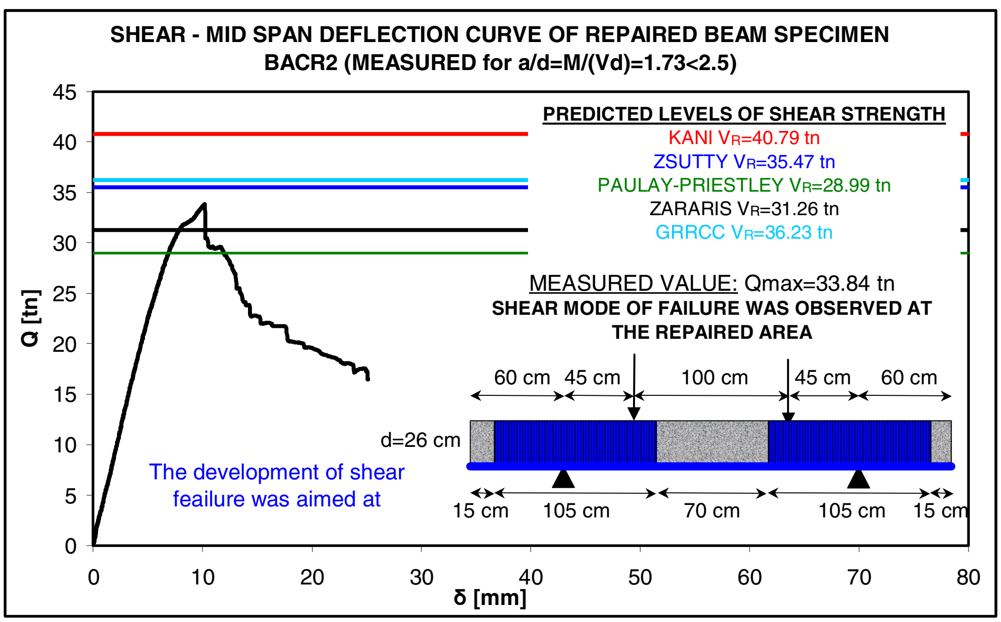

Figure 9. Comparison between observed shear demand and predicted shear capacity (BACR2)

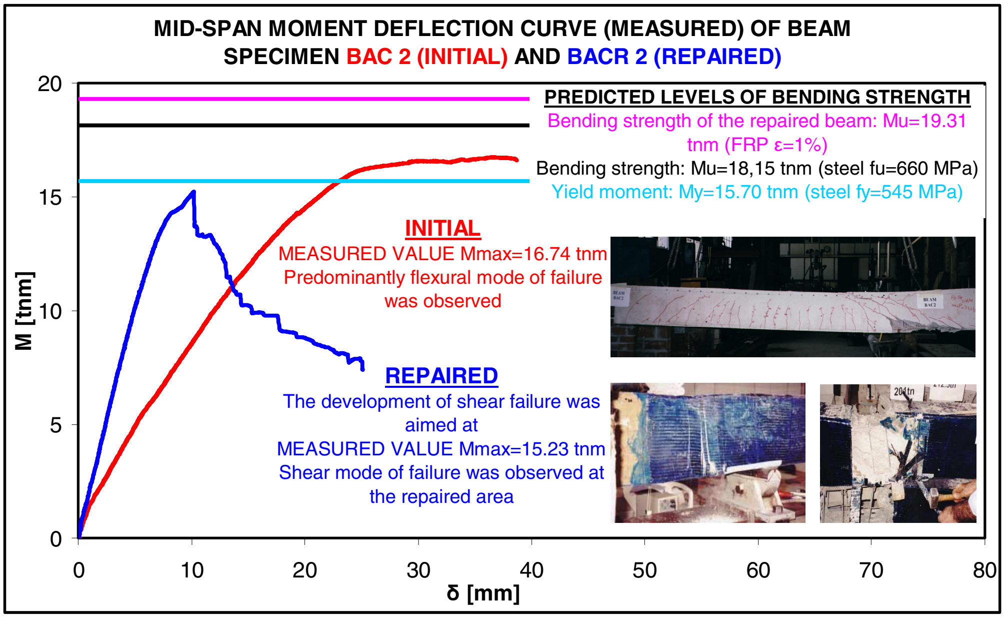

Fig. 10. Comparison between observed flexural demand and predicted flexural capacity (BAC2- BACR2)

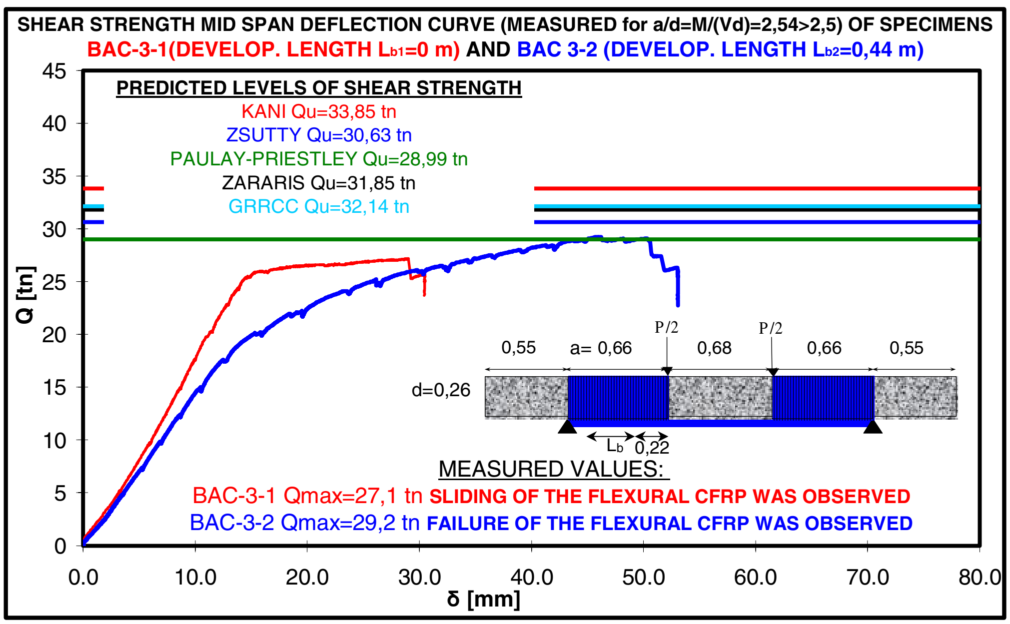

Figure 11. Comparison between observed shear demand and predicted shear capacity (BAC3-1, -2)

2.4.3. Specimen BAC3-1(slip of bottom side CFRP). Specimen Bac3-2 (fracture of bottom side CFRP).

In this virgin specimen (*BAC3-1)* CFRP was attached from the beginning in order to avoid shear failure and at the same time to upgrade the bending moment capacity by the bottom side attachment of the CFRP sheet. However, as already explained, this first attempt (BAC3-1) was partially successful due to the slip of the CFRP sheet. The second attempt (*Bac3-2)* was more successful as can be seen in figures 11 and 12. In figure 12 a ductile flexural behavior can be observed for BAC3-2 reaching the level of the predicted bending moment strength. At the same time, as indicated by figure 11, the upgraded shear capacity, predicted by all approaches, was higher than the shear demand. Only the shear capacity level predicted by Paulay and Priestly indicates that, at the final stages of the loading sequence for this specimen (BAC3-2), the shear capacity level is reached.

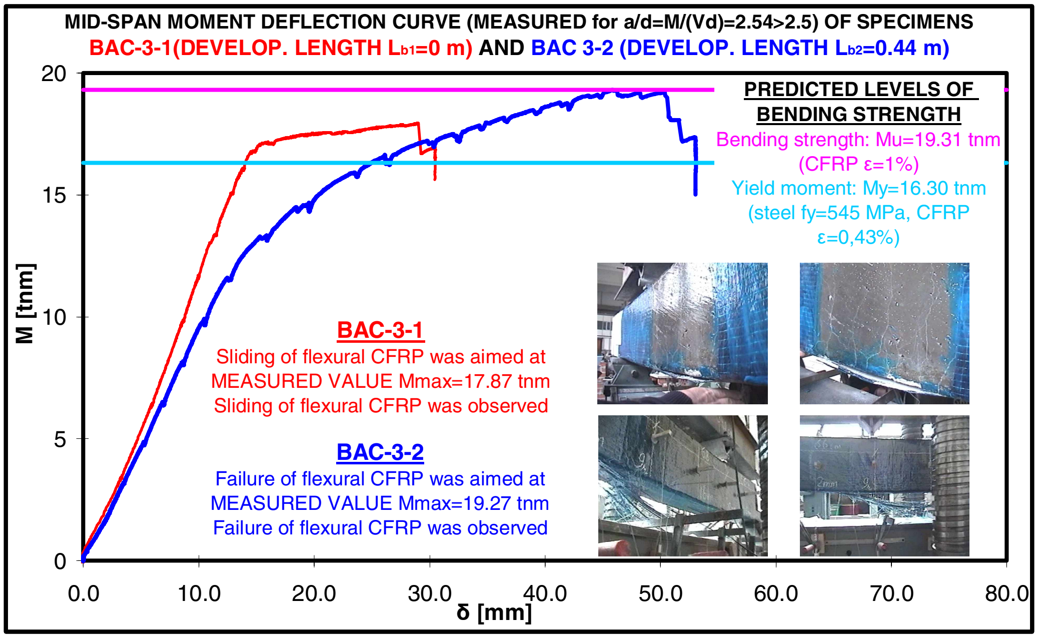

Figure 12. Comparison between observed flexural demand and predicted flexural capacity (BAC3-1 – BAC3-2)

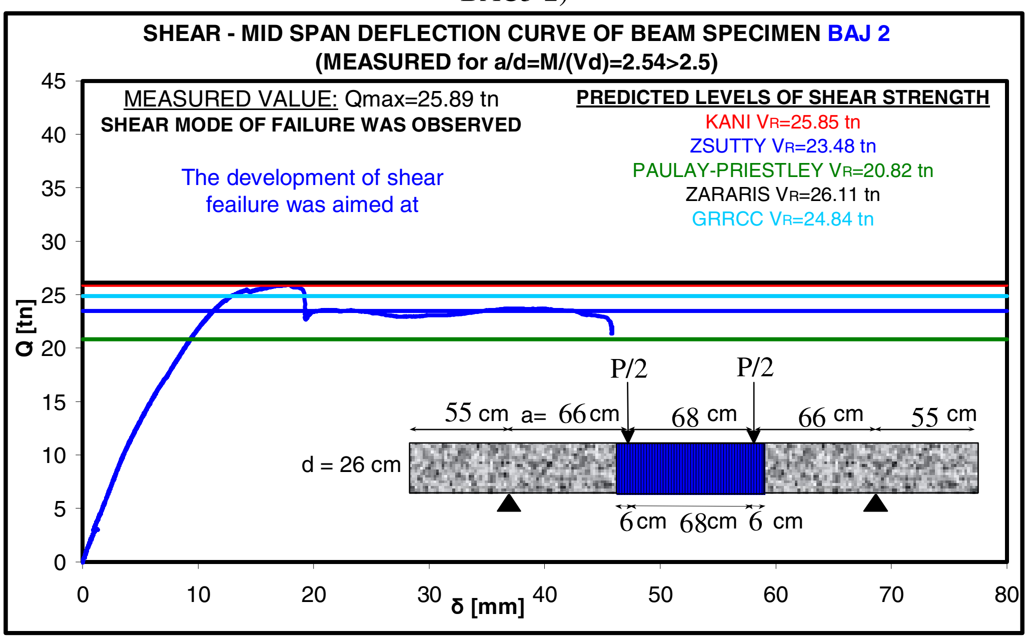

Figure 13. Comparison between observed shear demand and predicted shear capacity

2.4.4. Virgin specimenBAJ2 (scheme 3 central region)

This time the objective was to enforce the development of shear failure by upgrading the compressive strength of the concrete zone at the upper part of the central region of the specimen; this was done by confinement through the attachment of CFRP sheets according to scheme 3. The observed and predicted performance in this case is indicated by figures 13 and 14. The observed mode of failure was predominantly in shear. All approaches predict quite successfully this observed shear mode of failure (figure 13). It must also be noted that the M/Vd ratio in this case is equal to 2.54 (almost at the limit of 2.5). It can be seen that the shear capacity prediction of Paulay and Priestly is somewhat conservative. Moreover, the predicted bending strength is well above the bending moment demand (figure 14).

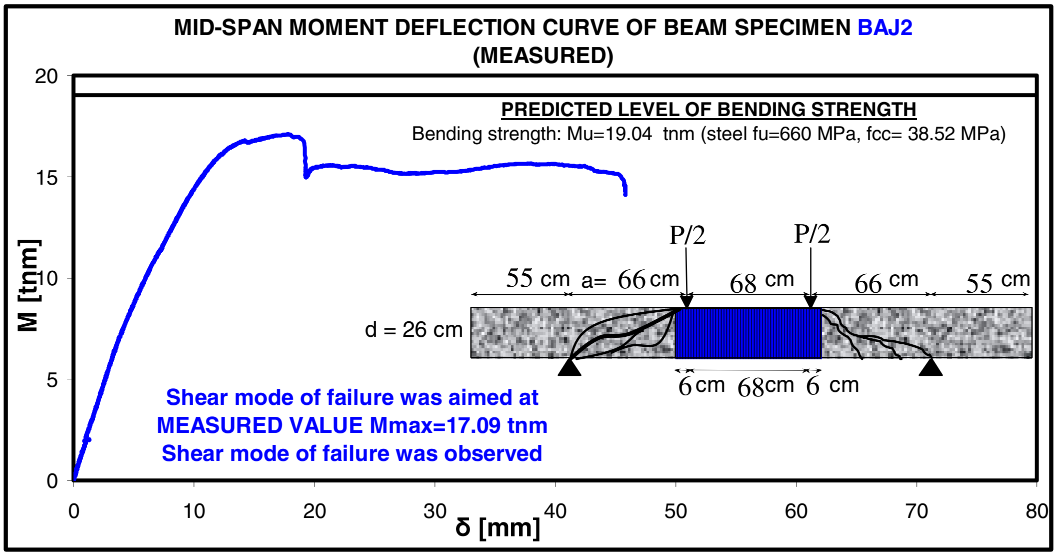

Figure 14. Comparison between observed flexural demand and predicted flexural capacity (BAJ2)

Table 5. Measured and predicted level of shear strength for beam specimen BAJR1 (a=0.90m).

PREDICTION OF SHEAR STRENGTH					EXPERIMENTAL MEASUREMENT	RATIO Exp/Pred
BASED ON	Vc [kN]	Vw [kN]	V_{FRP} [kN]	V_R[kN]	Qmax [kN]	Pmax/Pcr
Kani	69.87	146.12	80.22	296.21	201.11	0.68
Zsutty	66.85	146.12	80.22	293.19	201.11	0.69
Pauley-Priestley	58.06	146.12	80.22	284.40	201.11	0.71
Zararis	136.51	126.45	80.22	343.18	201.11	0.59
Greek R/C Code 2000*	103.55	131.51	80.22	315.28	201.11	0.64

* Without Safety Factors. This Greek Code is referred to as GRRCC when the corresponding results are plotted.

Table 6. Measured and predicted level of shear strength for beam specimen BACR2 (a=0.45m).

PREDICTION OF SHEAR STRENGTH					EXPERIMENTAL MEASUREMENT	RATIO Exp/Pred
BASED ON	Vc [kN]	Vw [kN]	V_{FRP} [kN]	V_R[kN]	Qmax [kN]	Pmax/Pcr
Kani	173.77	146.12	80.22	400.11	331.92	0.83
Zsutty	121.66	146.12	80.22	348.00	331.92	0.95
Pauley-Priestley	58.06	146.12	80.22	284.40	331.92	1.17
Zararis	137.06	89.44	80.22	306.72	331.92	1.08
Greek R/C Code 2000	281.08	131.51	80.22	492.81	331.92	0.67

* Without Safety Factors. This Greek Code is referred to as GRRCC when the corresponding results are plotted.

Table 7. Measured and predicted level of shear strength for beams BAC3-1and BAC3-2 (a=0.66m).

PREDICTION OF SHEAR STRENGTH					EXPERIMENTAL MEASUREMENT	RATIO Exp/Pred
BASED ON	Vc [kN]	Vw [kN]	V_{FRP} [kN]	V_R[kN]	Qmax** [kN]	Pmax/Pcr
Kani	105.69	146.12	80.22	332.03	286.45	0.86
Zsutty	74.13	146.12	80.22	300.47	286.45	0.95
Pauley-Priestley	58.06	146.12	80.22	284.40	286.45	1.01
Zararis	139.50	92.73	80.22	312.45	286.45	0.92
Greek R/C Code 2000*	103.55	131.51	80.22	315.28	286.45	0.91

* Without Safety Factors. This Greek Code is referred to as GRRCC when the corresponding results are plotted.
** The results from the measured response of beam BAC-3-2 are used (the largest between BAC3-1 and BAC3-2).

3. CONCLUSIONS

1. The employed CFRP technique, together with fast cured high strength concrete, was very successful in confining the rectangular column specimens damaged initially by axial compression. The repaired specimens, even without the participation of the longitudinal bars, exhibited very satisfactory axial compression behavior. This repair technique can be applied relatively fast and can be successful for short-term interventions in damaged columns, mainly providing the axial load capacity for permanent loads immediately after a strong earthquake. The predicted values of ultimate compressive strength agree reasonably well with the observed behavior.
2. The employed CFRP technique, together with fast cured high strength concrete, applied in a way to repair flexural or shear type of damage for beams, was quite successful in restoring or upgrading the desired shear or bending moment strength. Moreover, existing approaches can be used to predict the shear and bending moment capacities (including the contribution of CFRP) in such a way that the desired mode of failure does develop whereas the undesirable mode we are aiming to suppress is prohibited. This study demonstrated that, depending on the M / (V d) ratio value, the shear capacity prediction seems to be the one with the largest degree of uncertainty. Consequently, this uncertainty should be offset by a relevant safety factor.
3. The applied CFRP sheets must be ensured against slip failure. This can occur both in the case of attaching FRP sheets at the bottom side of a beam for upgrading the flexural capacity or in the case of applying FRP shear upgrading. In the present study the application of the shear upgrading was very easy as the CFRP could surround the beam from all sides; however, this will be prohibited by the presence of a slab in actual practical applications.

REFERENCES

1. G. N. J. Kani, «Basic Facts Concerning Shear Failure», J. ACI, Vol. 63, Jun. 1966, pp. 675-692.
2. S. Pantazopoulou, «Jackets of composite materials utilized to repair damaged reinforced concrete structural members”, Seminar May 2000, Technical Chamber of Greece. (in Greek).
3. T. Pauley, M. J. N. Priestley «Seismic Design of Reinforced Concrete and Masonry Structures», J. Wiley & Sons, INC USA 1992.
4. D. Stavrou, «Experimental and Analytical investigation of the repair and strengthening of simple R.C. structural members utilizing FRP’s”, Masters’ Thesis, Dept. of Civil Eng. 2002, (in Greek).
5. P. D. Zararis (2002) «Reinforced Concrete», Thessaloniki, (in Greek).
6. T. C. Zsutty, «Beam Shear Strength Prediction by Analysis of Existing Data», Journal ACI, Vol. 65, November 1968, pp. 943-951.
7. “Greek Code for Reinforced Concrete– GRRCC (ΕΚΩΣ 2000, in Greek).